Asymmetric Planetary Nebulae III
ASP Conference Series, Vol. XXX, 2004
M. Meixner, J. Kastner, and N. Soker eds.

Radio Cores of Bipolar Nebulae: Search for Collimated Winds

Ting-Hui Lee

Department of Physics and Astronomy, University of Calgary, Canada

Jeremy Lim, Sun Kwok[1]

Institute of Astronomy and Astrophysics, Academic Sinica, Taiwan

Abstract.

We present results of our search for collimated ionized winds in bipolar nebulae using the Very Large Array (VLA) and the Australia Telescope Compact Array (ATCA). Our search is motivated by the discovery of an ionized jet in the bipolar nebula M 2-9 (Lim & Kwok 2003) that may be responsible for sculpting the nebula's mirror-symmetric structure. To determine if such jets are a common feature of bipolar nebulae, we searched for optically-thick radio cores - a characteristic signature of ionized jets - in 11 northern nebulae with the VLA at 1.3 cm and 0.7 cm, and in 5 southern nebulae with the ATCA at 6 cm and 3.6 cm. Two northern objects, 19W32 and M 1-91, and two southern objects, He2-84 and and Mz 3, exhibit a compact radio core with a rising spectrum consistent with an ionized jet. Th 2-B exhibits a steeply falling spectrum characteristic of nonthermal radio emission. Here we present a preliminary analysis of these five radio cores and discuss the implications of our results.

1. Introduction

Bipolar nebulae are defined as axially symmetric planetary nebulae having two lobes with an 'equatorial' waist (Schwarz, Corradi, & Stanghellini 1992). In the context of the"generalized wind-blown bubble," a fast and spherically-symmetric wind from the central post-AGB star sweeps up a slowly-expanding axially-symmetric envelope previously expelled by the progenitor red giant star to produce a bipolar nebula. Such a model, however, can only produce bipolar nebulae with wide waists, not those with narrow "pinched" waists (Soker & Rappoport 2000, and references therein). Soker & Rappaport argued that the creation of bipolar nebulae with narrow waists requires a collimated wind, which in their model originates from a white dwarf companion accreting the wind of its red giant primary, i.e., a symbiotic star system. Such a collimated wind in the form of an ionized jet has indeed been discovered in the prototype narrow-waist bipolar nebula M 2-9 (Lim & Kwok 2000, 2003). The radio core of M 2-9 has a spectral

[1]Also Department of Physics and Astronomy, University of Calgary, Canada

index of 0.67, which is in nearly perfect agreement with the spectral index of 0.6 expected from an isothermal outflow expanding at a constant velocity and opening angle (Reynolds 1986). To determine if central ionized jets are a common feature of bipolar nebulae, we observed a total of 16 objects listed as bipolar nebulae with very narrow waists in Table 1 of Soker & Rappaport (2000). Our sample comprises 11 northern objects, IRAS 07131-0147, M 1-16, NGC 2818, NGC 6302, 19W32, HB 5, NGC 6537, M 3-28, M 1-91 M 2-48, and NGC 7026, observed with the VLA at 1.3 cm and 0.7 cm, and 5 southern objects, He 2-25, He 2-36, He 2-84, Th 2-B, and Mz 3, observed with the ATCA at 6 cm and 3.6 cm.

2. Results and Analysis

2.1. VLA Survey

We made the VLA observations in March 2002 when the telescope was in its A configuration. To correct for rapid tropospheric phase variations, we used fast switching with a calibration cycle time of just 2–3 minutes. The data were reduced and analyzed using the AIPS package developed by the National Radio Astronomy Observatory. We achieved an angular resolution of up to $\sim 0.08''$ at 1.3 cm and $\sim 0.04''$ at 0.7 cm.

We found that NGC 6302, Hubble 5, and NGC 6537 exhibit extended radio emission that could not be properly mapped due to the lack of short baselines in our observations. By contrast, 19W32 and M1-91 show a compact central source only at both 1.3 cm and 0.7 cm. No emission was detected from the remaining six objects. Note that this is the first time the centers of all these nebulae have been examined at such high angular resolutions at radio wavelengths.

To determine the flux densities of the radio cores observed in 19W32 and M1-91, we fit a two-dimensional Gaussian structure to the measurements by applying the task IMFIT to the clean map and OMFIT to the visibility data. We fit the entire dataset at 1.3 and 0.7 cm, and also a more restricted dataset at 0.7 cm chosen to have the same angular resolution as at 1.3 cm to check for a greater inclusion of any extended nebular emission in the larger synthesized beam. We found that both procedures gave the same results within measurement uncertainties. Thus, in Table 1, we list the results obtained by fitting the datasets over their entire uv range.

Table 1. Flux densities for compact cores detected with VLA

Object	Fitting Process	1.3 cm (mJy)	0.7 cm (mJy)	Spectral Index
19W32	Visibility fit	3.58 ± 0.18	6.18 ± 0.69	0.81 ± 0.18
	Map fit	3.48 ± 0.17	4.76 ± 0.57	0.47 ± 0.19
M 1-91	Visibility fit	2.97 ± 0.16	5.11 ± 0.39	0.79 ± 0.14
	Map fit	2.65 ± 0.15	3.97 ± 0.38	0.64 ± 0.17

The rising spectrum of both 19W32 and M1-91 suggest that their radio cores are produced by optically-thick free-free emission. Fits to the measured visibilities show that these cores are resolved along one dimension. If we assume a circularly uniform source of the measured dimensions, we deduce brightness

temperatures as listed in Table 2 that are a factor of a few below that expected for ionized winds (in the case of M2-9, $T_B \geq 4000$K). On this basis, we anticipate that the radio cores are noncircular, suggesting a collimated wind or jet. We plan observations at higher angular resolutions to properly map the structure of these radio cores.

Table 2. Deduced brightness temperatures for 19W32 and M 1-91

Object	Wavelength	Resolved Axis	Position Angle	T_B
19W32	1.3 cm	63 ± 11 mas	51° ± 19°	2150 ± 540 K
	0.7 cm	51 ± 10 mas	56° ± 46°	1650 ± 490 K
M 1-91	1.3 cm	77 ± 7 mas	86° ± 6°	1190 ± 170 K
	0.7 cm	34 ± 6 mas	58° ± 12°	3120 ± 810 K

2.2. ATCA Survey

We conducted the ATCA observations in March 2003 with the telescope in its 6-km configuration. The data were reduced using the MIRIAD reduction package. We attained an angular resolution of ∼3″ at 6 cm and ∼1.5″ at 3.6 cm.

We found He 2-36 to exhibit extended emission only, whereas He 2-84 and Th 2-B exhibit only a compact central source. Mz 3 show both compact and extended emission. No emission was detected from He 2-25. For He 2-84 and Th 2-B, we applied the task IMFIT to the clean map and UVFIT to the visibility data to determine the flux densities of their radio cores. In both cases, we assumed their radio cores to have a two-dimensional Gaussian structure. For Mz 3, the flux density was obtained only for the bright compact core in the clean map, as can be seen in Figure 1. The results are listed in Table 3.

Table 3. Flux densities for compact cores detected with ATCA

Object	Fitting Process	6 cm (mJy)	3.6 cm (mJy)	Spectral Index
He 2-84	Visibility fit	12.1 ± 0.16	9.2 ± 0.16	−0.47 ± 0.04
	Map fit	8.6 ± 0.06	7.7 ± 0.08	−0.18 ± 0.02
Th 2-B	Visibility fit	14.9 ± 0.12	8.2 ± 0.17	−1.01 ± 0.04
	Map fit	15.1 ± 0.09	10.1 ± 0.06	−0.68 ± 0.02
Mz 3	Map pixel sum	15.3 ± 0.14	18.3 ± 0.15	+0.35 ± 0.02

Two of the three radio cores have spectral indices significantly smaller than the value of −0.1 expected for optically thin free-free emission. However, these indices assume the flux measurements are of the cores only. If diffuse emission is present on scales the array can detect, it will contaminate these fluxes, perhaps even in different amounts at 3.6 and 6 cm. To guard against this possibility, we excluded short baselines that may be sensitive to extended emission, and also the long baselines at 3.6 cm to provide the same angular resolution as at 6 cm. The results obtained from the clean maps are listed in Table 4.

The difference in the core flux densities and resultant spectral indices evaluated using the different methods suggest that the emission comes a diffuse source and a compact source in the cases of He2-84 and Mz 3. In these two cases, the more careful analysis incorporating the same uv-coverage (Table 4)

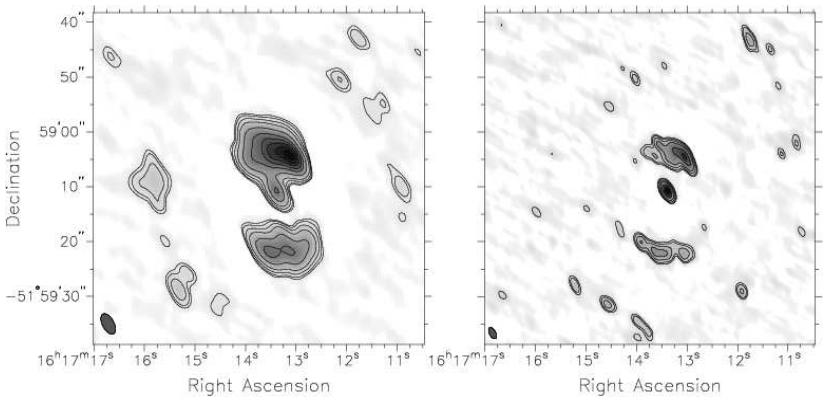

Figure 1. Radio map of Mz 3 at 6 cm (left) and 3.6 cm (right). The contours start at 3σ.

Table 4. Compact ATCA core fluxes vs. uv-range

Object	uv-range (kλ)	6 cm (mJy)	3.6 cm (mJy)	Spectral Index
He 2-84	50-100	1.83 ± 0.14	2.60 ± 0.10	+0.60 ± 0.15
	65-100	1.39 ± 0.16	1.89 ± 0.12	+0.52 ± 0.22
	75-100	1.08 ± 0.18	1.42 ± 0.15	+0.47 ± 0.34
Th 2-B	65-100	11.1 ± 0.16	5.7 ± 0.13	−1.13 ± 0.05
	75-100	10.8 ± 0.18	5.5 ± 0.16	−1.15 ± 0.06
Mz 3	45-100	13.3 ± 0.11	19.5 ± 0.11	+0.65 ± 0.02
	55-100	10.8 ± 0.14	20.3 ± 0.11	+1.07 ± 0.02

indicates that we have detected an optically-thick radio core. For Th 2-B, in both analyses we derive a spectral index close to −1, implying a nonthermal emission mechanism. We plan observations at higher angular resolutions, as is possible with the newly-commissioned 12 mm and 3 mm systems at the ATCA, to better understand the nature of these radio cores.

Acknowledgments. This work is supported by a grant from Natural Sciences and Engineering Research Council of Canada.

References

Lim, J., & Kwok, S. 2000, in ASP Conf. Ser. 199, "Asymmetric Planetary Nebulae II: from Origins to Microstructures," eds. J. Kastner, S. Rappaport, & N. Soker (San Francisco: ASP), 259

Lim, J. & Kwok, S. 2003, in ASP Conf. Ser. 303, "Symbiotic Stars probing Stellar Evolution," eds. R. L. M. Corradi, J. Mikolajewska, & T. J. Mahoney (San Francisco: ASP), in press

Reynolds, S. P. 1986, ApJ, 304, 713

Soker, N. & Rappaport, S. 2000, ApJ, 421, 259

Schwarz, H. E., Corradi, R. L. M. & Stanghellini, L. 1992, A&AS, 96, 23